

Design of the Chassis and Locomotion System for a Mobile Robot

Andre Webber-LaHatte

Abstract—A new drive chassis and locomotion system is designed for MARVIN (Mobile Autonomous Robotic Vehicle for Indoor Navigation), a human-robot interaction (HRI) research platform. Design was conducted with a focus on power consumption, waste reduction, stability, and adaptability, in line with the project’s sustainability goals. It successfully met design requirements and displayed power usage allowing operation times comparable with similar platforms. Test results demonstrated its ability to travel at both slow and medium to fast walking paces on different drive terrains. Safety is ensured, with its ability to execute a software emergency stop within 1 m. Future work will concentrate on refining locomotion control, enhancing safety features, and implementing autonomous capabilities, further expanding MARVIN’s potential for various applications and environments.

I. INTRODUCTION

MARVIN is a humanoid robot platform that is purposed for autonomous navigation within areas of Victoria University of Wellington’s (VUW) Kelburn campus. This is a high-profile robot that has been featured in a Dominion Post article [1], One News [2], and is on the cover page of VUW’s “Victorious” magazine, summer 2006 edition [2]. MARVIN’s main function is as a research platform for HRI, a university guide, and a security device [3]. Presently MARVIN is lacking the hardware and control systems necessary for mobility.

A. Previous Implementations

The most recent drive system employed is the Segway robotic mobility platform (RMP) [3]. This platform is a differential drive with self-balancing capabilities. Concerns with this platform, involve health and safety, development issues, and difficulties in maintenance. In the event of power failure, the platform will lose its self-balancing capabilities and fall over. Difficulty with this platform has been faced by students taking on development projects, one experiencing unexpected shutdowns of the platform. Maintenance of the platform requires sending it to Segway and will incur a fee. A decision to design and implement a system that can be maintained at VUW.

Before the Segway RMP, a dual castor differential drive system was used for mobility [4]. This system was the original drive system employed by MARVIN and was working correctly before the implementation of the RMP [5]. The drive chassis for this implementation, shown in figure 1, is constructed with a steel base, and extruded aluminium angle bar form the height and shape.

This project was supervised by Dale Carnegie, and Hamish Colenso.

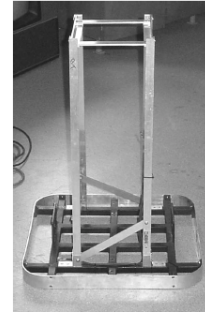


Fig. 1. MARVIN’s original drive chassis [4]

B. Sustainability

Sustainability has become a central concern in modern engineering, impacting both the environment and the long-term functionality of robotic systems. In the case of MARVIN, a commitment to sustainability has driven design decisions made in the project. The following aspects describe the project’s sustainability approach:

- **Energy Efficiency:** Steps are taken to minimise energy consumption through the choice of lightweight components, such as the aluminium structure of MARVIN’s chassis, and the use of lithium batteries. Additionally, a motor driver is implemented that will enable regenerative braking.
- **Modularity:** This considers the next steps of the project. Designing a modular platform allows future developments to be made with little to no modifications, aiding in New Zealand’s sustainability objectives concerning waste reduction [6]
- **Re-use** A re-use goal is a large part of this project, with inherited components from prior implementations used in this design where appropriate as part of a waste reduction objective.
- **Longevity** A lightweight chassis is designed to help reduce strain on components, allowing them to last longer.

C. Problem

The drive chassis in MARVIN’s most recent implementation is no longer functional. Additionally, there is no central controller implemented, nor batteries. This necessitates the design of a new chassis and locomotion system that will allow MARVIN to travel within VUW’s Kelburn Campus. Notable characteristics of this operational environment are as follows:

- Carpet floors
- Vinyl floors

- Lips on carpet/vinyl junctions (maximum 8 mm high)
- Corridors 1.5 m in width with 90° turns
- Doorways 800 mm in width

D. Design Requirements

- Marvin must be capable of moving at slow, medium, and fast walking paces, defined as 0.8 ms^{-1} , 1.3 ms^{-1} , and 1.5 ms^{-1} respectively [7]. Previous implementations have limited MARVIN's velocity to 1.4 ms^{-1} [8]. Thus MARVIN must be capable of moving at both 0.8 ms^{-1} , and 1.4 ms^{-1} on carpet and vinyl.
- MARVIN must not cause damage to carpet while in operation
- MARVIN must be capable of executing 90° turns in corridors 1.5 m in width.
- MARVIN must be able to traverse 8 mm high lips
- MARVIN's computational power should be sufficient for autonomous navigation
- MARVIN must be sufficiently stable to achieve stopping distances within 1 m without falling over.
- MARVIN must be able to drive through doorways 800 mm wide
- MARVIN should be capable of achieving comparable run times with similar platforms
- Software should implement interfacing with Torso hardware

II. INHERITED PLATFORM

A. MARVIN's Torso

The inherited torso, shown in figure 2, is the primary component of MARVIN that enables HRI and has been used across multiple implementations. The ability to change the position of its head and torso, and change eye colour, enables the emulation of human emotions. The torso assembly consists of the base plate, weighing 10 kg, and the torso itself, weighing 13 kg. The torso assembly has a maximum total height of 1 m. Actuators through which the torso achieves its functionality are:

- Linear Actuators: Three for torso position, one for head height.
- Servo motors: Used for nodding, tilting, and shaking the head.
- RGB LEDs: Two RGB LEDs act as MARVIN's eyes
- Headlamp: Serves as an additional light source.

Torso control is achieved through four control boards, the torso control board (TCB), the RGB LED Control Board, and two Linear Actuator Control Boards (LACB). The control flow for torso hardware is shown in figure 3.

MARVIN Power Supply Unit (PSU)

The power supply board integrates 3 switching regulators, which are all capable of converting input voltages in the range 18 V to 36 V [9]. Output voltages are 5 V, 12 V, and 24 V, with current capacity 10 A, 14.7 A, and 14.5 A respectively. This board contains dedicated outputs for various components, including the TCB, RGB LED Eye Control Board, LACB, audio, lidar, sensors, IR, and auxiliary sensors. Though some connectors have been repurposed.



Fig. 2. MARVIN's torso

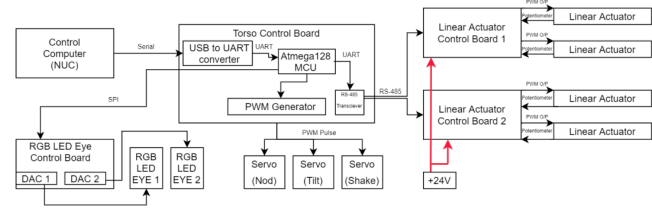


Fig. 3. Block diagram of torso control stack

B. Motors, Gears, and Drive Wheels

The motors, gears, and drive wheels are inherited from a previous implementation (before the RMP). Motors are brushed DC motor gearbox assemblies, with a 17:1 worm gear configuration between the motor shaft and output shaft. Inherited gears consist of a 24-tooth spur gear, and a 75-tooth ring gear (within the drive wheel), providing a 3.125:1 gear ratio. Inherited drive wheels are tubed pneumatic wheels, with a 165 mm radius. Spur and ring gears are module 2, and require a 51 mm centre distance.

C. Sensors

1) *Ultrasonic Sensors*: Five LV-MaxSonar-EZ4 ultrasonic sensors are inherited [10]. The data sheet states a 0 m minimum, and 6.45 m maximum ranging distance. These sensors have 7-pin connectors, two of which are for power, the function and name of the others follows:

- TX: Output pin, emits a $20 \mu\text{s}$ pulse to indicate a reading is finished, or acts as a serial line, outputting the range value in RS232 format.
- BW: Input pin used to select the mode used by TX
- PW: Output pin that sends a pulse width representation of range using $124 \mu\text{s}$ per inch
- AN: Outputs an analogue voltage representation of range at $V_{\text{cc}}/512 \text{ V}$ per inch. When using a 5 V supply, distance in cm can be found using $d = 1.27v$, where v is the voltage output by AN.
- RX: Input pin, a $20 \mu\text{s}$ pulse on this pin will trigger the sensor to range or can be held high for continuous ranging.

2) *PSD Sensors*: Four Sharp 2Y0A710 sensors are inherited, with a minimum 1 m, and maximum 5.5 m sensed distance [11]. These sensors range continuously when on, and

output an analogue voltage representation of distance. Using information from [12], the distance in cm can be found by $d = 137.5/(v - 1.125)$, where v is the analogue voltage output of the PSD sensor.

3) *Sensor Board*: A sensor board is inherited that is designed as a shield for an Arduino Mega. This board acts as an interface between sensors and a main control computer via a USB connection with the Arduino. The sensor implements connections for a variety of sensing and control devices, including the PSD and ultrasonic sensors. Other sensing and control devices are not discussed in this report as they are not part of the inherited platform. Connections between each sensor board connection and relevant Arduino pins were determined through the use of a continuity tester. This information is used to determine the hardware configuration used by the ultrasonic sensors. A daisy chain configuration is used, shown in figure 4, reading the AN pin of each sensor to determine the sensed range. A GPIO pin is used to trigger ranging on the first sensor in the chain, and another listens for the last sensor to emit its TX pulse. Additionally, the analogue pins associated with each PSD and ultrasonic sensor are determined.

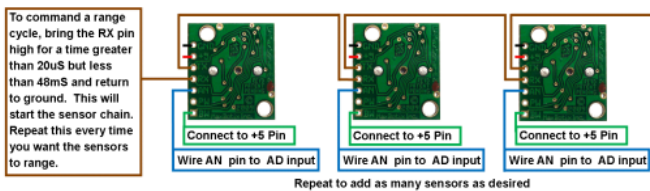


Fig. 4. Sequential daisy chain configuration of ultrasonic sensors [10]

III. BACKGROUND RESEARCH AND RELATED WORKS

A. Locomotion

MARVIN's indoor operating environment has no rough terrain and is mostly flat, obstacles consist of 8 mm lips. Using legged configurations provides no advantage in MARVIN's operating environment, and will increase both mechanical complexity and power requirements [13]. This section focuses on wheeled robot configurations. Wheeled robot designs are usually simpler than legged robots, and are often very efficient in comparison [13]. Wheeled configurations also provide an advantage in terms of stability [14]. Balance and stability of wheeled robots is typically achieved by ensuring sufficient points of contact with the ground [14]. Three contact points are enough to guarantee stability, greater stability can be achieved by with more contact points, though requires a suspension system for use on uneven terrain.

B. Wheels

The four main categories of wheel are; standard, castor, Swedish (or "mecanum"), and spherical [13]. Standard wheels are either fixed, where orientation relative to chassis cannot be changed, or steered which can rotate on a vertical axis that intersects the rolling axis. Unlike steered standard, castor wheels have a vertical rotation axis offset from the rolling axis, allowing compensation for lateral forces. Swedish wheels use

passive rollers at either 90° or 45° angles and can achieve omnidirectional motion. Spherical wheels are ball casters and have no primary axis of rotation. All but standard wheels are considered omnidirectional, and impart no kinematic constraints on a robot chassis.

C. Drive Configurations

Omnidirectional Configurations

Omnidirectional configurations are by definition highly manoeuvrable, as they allow a robot to move in any direction on a horizontal plane. A description of two omnidirectional drive configurations follows.

- **Synchro drive** [13]: This configuration uses three wheels driven synchronously with a single motor, and oriented synchronously with another. This is the most easily controlled omnidirectional configuration, however requires a complex power transmission system.

- **Swedish omni drive** [13]: Comes in two types, three wheeled 90°, or four wheeled 45°. In these configurations each wheel is independently driven, requiring a less complex mechanical drive system than synchro drive, but a more complex control system. These configurations allow for on-the-spot rotation. Driving Swedish omnis in a straight line poses a challenge due to drift in dead reckoning and slippage.

Differential Drive

This drive system uses two independently controlled fixed standard wheels [13]. To drive in a straight line, each wheel must be driven in the same direction, at the same speed. Turning on the spot is achieved by driving each wheel at the same speed, in opposite directions. Arbitrary motion can be achieved with varying combinations of wheel speed and direction. This configuration has low mechanical complexity and is easy to control. Potential irregularities between each wheel can make driving in a straight line difficult. Differential drives usually employ the use of one or two free-moving omnidirectional wheels to ensure stability.

Tricycle Configuration

This configuration uses two rear wheels, and a single actively steered front wheel [13]. The drive is provided either with the rear or front wheels. This configuration cannot achieve in-place rotation. Controllability is simple and mechanical complexity is low, however, the centre of gravity moves away from the wheels during acceleration making this configuration prone to slippage. Additionally, the steered wheel can impose damage to surfaces if turned while the robot is stationary [4].

Quad Steer

These come as either two-wheel steering or four-wheel steering [4]. Both two and four-wheel steering require a large drive motor, and a differential gear system for power transmission, making it mechanically complex compared with the tricycle. When turning, the inside wheel must be turned to a sharper angle than the outside to reduce slippage, adding complexities to control.

A visualisation of the quad steer, tricycle, and differential drive configurations is shown in figure 5.

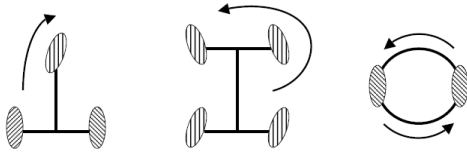


Fig. 5. Tricycle (left), Quad 4-wheel steer (centre), and differential (right) drive configurations [13]

D. Motors

This section discusses motor types and feedback options for motor control. MARVIN's mobility necessitates the use of batteries, which provide a DC supply, as such, AC motors are not considered.

DC Motors

DC motors can have their speed adjusted by changing the applied voltage. They have an equivalent circuit, shown in figure 6 [15], where V is the voltage on the motor, R is the armature resistance, L is the motor inductance, and E is the back EMF. DC motors have two constants associated with them, the back EMF constant, k_e and the torque constant k_T . These constants describe the proportions; rotational velocity (rad/s) to back emf (V), and current (A) to torque (Nm). Where standard international units are used, $k_e = k_T$, allowing the use of k , the motor constant. With a known motor constant, the voltage and current to operate at a set point speed and torque can be determined.

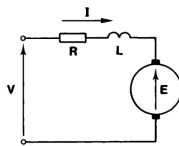


Fig. 6. Equivalent circuit of a DC motor [15]

Brushed DC Motors

Brushed DC motors consist of a rotating armature (the rotor) and a stationary set of either permanent magnets or electromagnets (the stator) [16]. When a current is applied to the motor, a magnetic field is created in the armature. The interaction between the armature and stator magnetic fields generates a torque, causing the rotor to rotate. The rotation of the rotor causes electrical connection to be constantly broken, and made through a commutator and carbon brushes. The direction of rotation can be changed by reversing the polarity of the applied DC.

Brushless DC Motors

Brushless DC (BLDC) motors place armature windings in the stator and use permanent magnets in the rotor [16]. Instead of using brushes and commutators, BLDC motors employ electronic controllers that rapidly switch the direction of current flow in the stator windings. This switching creates a rotating magnetic field in the stator that interacts with the permanent magnets in the rotor, generating a torque, and resulting in rotation. BLDC motors offer several advantages over brushed motors, including higher efficiency, longer lifespan, higher torque-to-weight ratio, and greater speed control accuracy.

Motor Feedback

Specific motor speeds can be achieved through feedback and control. Feedback is achieved with a motor encoder [17]. Generally, there are two types of motor encoders, incremental and absolute.

Incremental encoders use either optical or magnetic sensors to output several pulses per revolution [17]. They come in either single line or 2 lines of pulses (quadrate), where quadrate encoders can be used to determine both speed and direction.

Absolute encoders output a unique digital word based on the position of the motor shaft [17]. They achieve this using 2 concentric disks, one fixed, the other moving with the shaft. The advantages of absolute encoders over incremental encoders are accurate motion detection and better startup performance and recovery in system failure (where position control is required).

E. Case Study

This section gives descriptions of three robots. Two operate as HRI platforms and are assessed for functionality and performance. The third is assessed for the design and structure of its chassis.

1) *Jinny*: Jinny is a differential drive robot tour guide developed with a focus on HRI and autonomous navigation [11]. Jinny can accelerate at 0.5 ms up to a maximum speed of 1 ms⁻¹, is 1.5 m tall, with a radius of 0.6 m and has an 8-hour operating time. Operation of Jinny is handled by 3 on board computers; 2 Pentium-IV PCs for navigation and HRI, and a Pentium-III DOS PC for motion, connecting to the other computers via serial. Figure 7 gives an image of Jinny.



Fig. 7. Picture of Jinny [18]

2) *Ari*: Ari is a high-performance robot designed for HRI and support within the medical industry [19]. Ari uses a dual castor differential drive system and is capable of travelling at speeds up to 1.5 ms⁻¹ with an 8 to 12-hour battery life. Ari is capable of autonomous navigation through the use of Robotic Operating System 2 (ROS2), running on Intel i5 cores, using up to 32 GB of RAM. Figure 8 shows an image of Ari.

3) *AuckBot*: AuckBot is an omnidirectional, heavy-duty robotics research platform developed by the University of Auckland [20]. Auckbot makes use of t-slot aluminium extrusion to construct its chassis. This platform is observed to handle the weight of an adult human without exhibiting any bending or flexing of the chassis, nor impact to velocity



Fig. 8. Picture of Ari [19]

or manoeuvrability. Additionally, this platform makes use of ROS2 for control of its components.

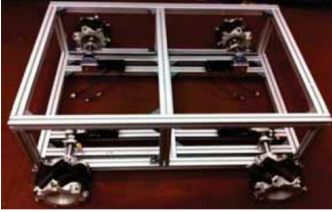


Fig. 9. Picture of AuckBot [20]

IV. DESIGN AND IMPLEMENTATION

A. Drive Configuration

With considerations made into MARVIN's operating environment, it has been determined that a differential drive configuration is the most appropriate for this application. The 0 turning radius ensures MARVIN's capability to navigate 90° angle turns in 1.5 m width corridors, and enables MARVIN to alter its trajectory on the spot without causing damage to carpets.

Implementation of this drive configuration uses MARVIN's original drive wheels, which are observed to have sustained little to no damage in their lifetime. Casters are chosen to handle a 90 kg load based on a previous implementation [8]. The casters are made from an elastic rubber material, with mounting plates that allow for approximately 1 mm of vertical travel to help absorb shocks when traversing the lips present in MARVIN's operating environment.

Kinematic equations for a differential drive configuration are determined using chassis width, W and wheel radius, r [21]. Given a tangential, V , and rotational ω_z velocity, left and right wheel velocities ω_L and ω_R are found using equations 1 and 2. Given ω_L and ω_R , V , ω_z are found using equations 3 and 4. These equations can be used to implement locomotion control and odometry.

$$\omega_L = (V - (\omega_z \times W/2))/r \quad (1)$$

$$\omega_R = (V + (\omega_z \times W/2))/r \quad (2)$$

$$V = r \times (\omega_L + \omega_R)/2 \quad (3)$$

$$\omega_z = r \times (\omega_R - \omega_L)/W \quad (4)$$

B. Electronics and Electrical

1) *Motor selection:* Motors must be capable of producing torques necessary to operate at medium to fast walking paces in MARVIN's operating environment, within any constraints introduced by motor drivers and batteries. In line with the project's re-use and sustainability goals, a decision is made to re-purpose the inherited motors described in section II. Testing is conducted on the motors to determine their suitability, initially finding each motor to have an armature resistance of 1.2 Ω and 1.6 Ω , further testing required encoders, and a motor driver. Battery, motor drive, and encoder selection are conducted under the assumption that these motors will work. Further testing is enabled with the possession of these components and is described later in this section.

2) *Battery Configuration:* Battery selection is driven by the following specifications and requirements:

- **Motor Voltage:** The inherited motors are rated to operate at 24 V [4].
- **Motor Current:** The inherited motors are stated to draw 10 A at peak speed [4].
- **Inherited PSU:** The inherited power supply unit incorporates three DC-DC converters able to take in inputs ranging from 18 V to 36 V [9].
- **Battery Weight:** Lightweight batteries are preferred in line with the project's energy efficiency and sustainability goals.

The chosen battery configuration is two 12.8 V, 25 Ah, lithium iron phosphate (LiFePO₄) batteries, wired in series. The discharge curve of these batteries, shown in figure 10, shows the batteries will supply 25.6 V to 26.2 V in a series configuration, which is within the operating range of the inherited PSU. While this is larger than the motor's rated voltage, it is assumed the required duty cycle will ensure the average voltage to the motors is less than 24 V.

Additionally, LiFePO₄ batteries are chosen for their lightweight and safety, being less prone to thermal runaway than other lithium batteries [22].

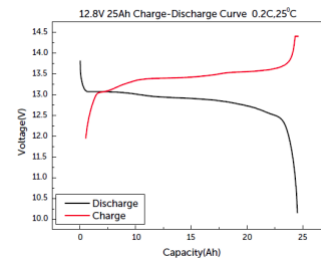


Fig. 10. Characteristic curve of MARVIN's batteries [23]

3) *Motor Driver Circuit:* The motor driver circuit is responsible for power delivery and control of the motors. This circuit must allow for independent closed-loop control of each motor, and implement an emergency stop. This circuit should also be capable of operating in the voltage range supplied by the batteries.

A Basic-micro dual channel motor driver is chosen (named Roboclaw) [24]. This device operates in the range of 7 V, to 34 V, so is compatible with the chosen batteries. It

implements firmware for performing independent closed-loop control of two motors. It is also equipped with safety features that will disable the motors if user-defined current, voltage, and temperature limits are exceeded. Sensor information can also be requested by a controller communicating with the Roboclaw via USB. For feedback, the Roboclaw incorporates inputs for two quadrature encoders and can read up to 19.6 million pulses per second.

The choice to implement the Roboclaw motor driver is also driven by the project's sustainability objectives. It is used on other robotic platforms at VUW, thus university technicians already have a working knowledge. This driver also has regenerative braking capabilities, which allow for improved energy efficiency. For the use of regenerative braking, the series battery configuration requires the design of external charge-balancing circuitry, beyond the scope of the project. A recommended voltage clamp circuit is implemented which is used to sink excess power to a resistor and prevent overloading the batteries during braking.

Additionally, a model is selected to handle the potential stall current of each motor continuously, which is found to be 22 A based on armature resistance. Roboclaw offers 30 A per channel, and 45 A per channel models, the 45 A rated model is selected to provide a safety margin.

An incremental quadrature encoder is chosen for feedback, to be fit onto each motor's output shaft. These encoders output 2000 pulses per revolution [25]. With the 1:3.125 gear ratio between the inherited spur gears and inherited drive wheels, and 1.4 ms^{-1} (medium walking pace) specified max velocity, these encoders will output approximately 8500 pulses per second, well below the 19.6 million pulses per second the Roboclaw can read.

A power switch and fuse are connected between the battery and the motor driver, with a high current diode to allow for power flow back to the battery in the event the fuse is blown. A hardware emergency stop switch is also implemented, enabling operators to cut power to the motors if necessary. This makes use of a normally open spring-loaded switch, with a 3D printed wedge and mount. The emergency stop assembly is shown in figure 11.

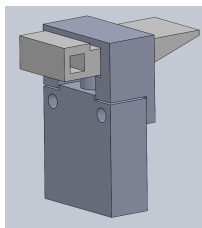


Fig. 11. Emergency stop stitch assembly

For powering the Roboclaw electronics, a 12 V line from the inherited PSU is used as the logic battery (LB) connection, which is used as the input to a linear regulator. Using 12 V rather than battery voltage on the Roboclaw's (LB) input, regulator losses are reduced, improving energy efficiency.

An electrical schematic of MARVIN is shown in figure 12. The schematic only shows electrical connections, omitting

signal connections (except the clamping resistor circuit signal) such as encoders, and USB.

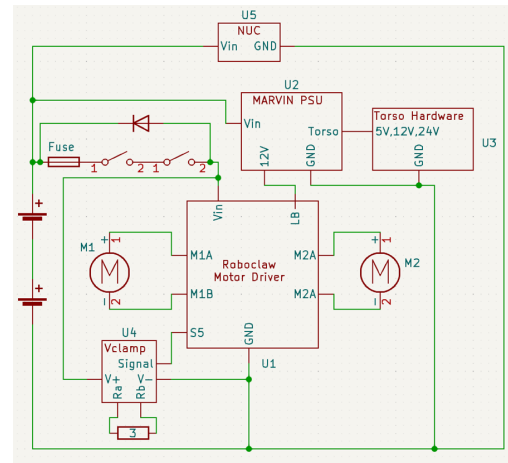


Fig. 12. Electrical Schematic for MARVIN

4) *Motor Testing:* Testing of the motors is done based on the DC motor equivalent circuit, shown in figure 6 in section III, D, to determine the motor constant for each motor.

A testing circuit is set up, shown in figure 13, note that the encoder connections are implicit. By recording the current, and voltage to each motor, at multiple set-point speeds, the motor constant is estimated. To estimate the torque loading on each motor, rolling resistance is used. Engineering toolbox gives the rolling resistance coefficient for bicycle tyres on concrete as 0.002 [26], this is taken as the rolling resistance of MARVIN's wheels on vinyl. The rolling resistance coefficient for rubber tyres on carpet is estimated using data from [27]. The force required to move a rubber tyre wheelchair with a 70 kg load averaged across different carpet types [27] is 5.5 N. Rolling resistance coefficient for rubber tyres on carpet is estimated at 0.08, this figure is used as the basis for determining motor suitability. Based on a prior implementation of MARVIN weighing 90 kg, this requires 7.2 N to move at a constant velocity, translating to approximately 0.2 Nm of torque on the output shaft of each motor. Additionally, the no-load torque for each motor operating at 26.5 rad/s (required rate to drive MARVIN at a medium to fast walking pace) is approximately 0.9 Nm (on the output shaft), thus each motor will see approximately 1.1 Nm when travelling at a fast walking pace on carpet.

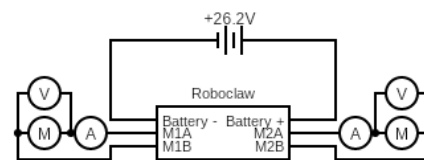


Fig. 13. Circuit Diagram of motor testing setup

According to test results and torque estimates, each motor requires a current 2.2 A, with an applied 19.1 V to operate at a fast walking pace on carpet. This corresponds with a duty

cycle of 73%, and a 3.2 A current draw from the batteries. These figures are well within the operating capabilities of the batteries and motor drivers, allowing sufficient headroom to account for any potential losses the testing ignored.

5) *Main Controller Selection*: The selection of the main controller is guided by the following requirements:

- **Interfacing**: Must be capable of interfacing with the TCB, sensor board, and Roboclaw motor driver.
- **Future Developments**: Must account for intended future developments, primarily regarding autonomous navigation.

The Intel NUC10i5FNH is equipped with Intel i5 quad-core processors and 16 GB of RAM. The computational power is comparable to that used by Ari [19], which is capable of autonomous navigation. Additionally, it possesses 3 USB ports, which can be used for interfacing with the drive, torso, and sensor hardware. Figure 14 gives a high-level view of the data connections used by MARVIN. For more information on torso control and the sensor board connections, refer to section II.

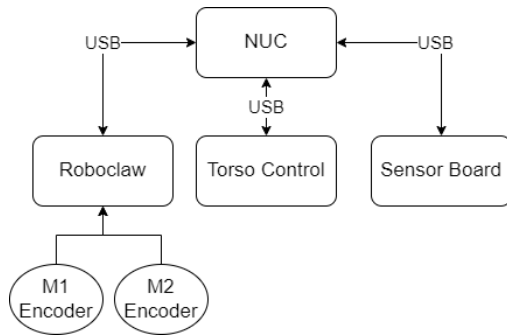


Fig. 14. High-level block diagram showing MARVIN's data connections

6) *Power Consumption and Run time Estimation*: An estimation of the power draw and run time is based on a worst-case scenario for each introduced component. The Roboclaw's linear regulator is rated for 3 A [24], the motors require 3.2 A from the battery, and the NUC's processor has a documented 39 W power draw under demanding workloads [28]. A bar graph showing the estimated current drawn by each introduced component is shown in figure 15 assuming a 26.2 V battery supply. As worst case figures are used, switching converter losses provided 12 V to the Roboclaw, and torso idle draw are ignored. This data gives an estimated run time of 4 hours based on 25 Ah batteries, assuming constant mobility on carpet.

C. Chassis

The chassis serves as the foundation upon which the locomotion system, and inherited torso and electronics systems are integrated. This section outlines the specifications, constraints, and design considerations for the chassis, along with the rationale for selecting a T-slot extruded aluminium (referred to as aluminium extrusion from here on) bolt-together solution.

1) Chassis Design Specifications:

- **Height**: The chassis must be a maximum of 1.7 m tall with the head height fully extended. This specification is

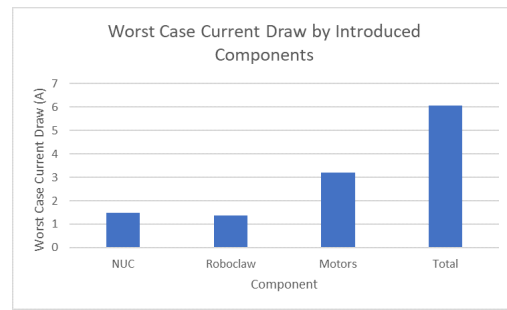


Fig. 15. Worst case current drawn by introduced components

driven by MARVIN's intended use as a research platform for HRI, the average height of men and women in NZ (1.78 m, and 1.65 m respectively [29]), as well as discussion with the project supervisor, Dale Carnegie, who is also a major stakeholder.

- **Electronics Integration**: The chassis must provide ample space and mounting solutions for both existing and new electronics, and cable requirements. Considerations must be made on the placement of electronics (including batteries and motors) to optimise weight distribution and stability.
- **Doorway Compatibility**: The chassis must be designed to fit through a standard doorway with a width of 800 mm. It is decided to ensure a mean clearance of 95 mm on either side of MARVIN as a safety margin, constraining the total width to 610 mm.
- **Rigidity**: The chassis needs to be a rigid structure to ensure stability and minimise wobbling during robot operation.

2) **Design**: Aluminium extrusion is chosen as the material used to form the chassis structure, which is proven to exhibit sufficient strength and rigidity to support the weight of MARVIN's torso and other components [20]. This decision is also largely driven by the project's sustainability objectives. A lightweight frame offers a greater energy efficiency, which aligns with New Zealand's (NZ) sustainability goals [6] by placing less demand on electrical energy generation, allowing a higher penetration of renewable energy [30], albeit on a small scale. Additionally, a lightweight chassis further aligns with NZ's sustainability goals by contributing to the extended longevity of components, reducing future waste. Lower energy consumption for mobility allows a greater operating time, requiring fewer cycles of the batteries in a given period, and results in smaller currents to the motors and motor driver. The mechanical strain on the gearing is also minimised. Lastly, the modularity offered by aluminium extrusion allows future developers to integrate additional components such as sensors with little to no modifications to the existing design.

The final design of the chassis implements 30x30 mm aluminium extrusion as the main support structure, as well as 3 mm aluminium plate on the top, bottom and sides. The use of aluminium plate increases the overall rigidity [5] [31], and provides mounting points for batteries, motors, wheels, and the inherited torso. The design process began with the mounting plate for the motor and wheels, this informs the

length of extrusion required to achieve a 1.7 m total height, and the placement of batteries that will balance the mechanical load on either side of the drive axis.

Mounting Plate for Motor and Wheel

The design of the mounting plates is guided by dimensions shown in Figure 16, a technical drawing of the motor, and Figure 17, a technical drawing of a model of the drive wheel. The internal ring gear on the wheel is 23 mm deep, with a mounting point in the centre that extrudes 32 mm from the face of the ring gear. The considered dimensions from figure 16 are as follows:

- The output motor shaft is 60 mm
- The encoder, encoder mount, and bearing cover use 19 mm of this length
- The output motor shaft is 72.5 mm above the bottom of the motor
- The motor's estimated COM is 95 mm from the motor shaft

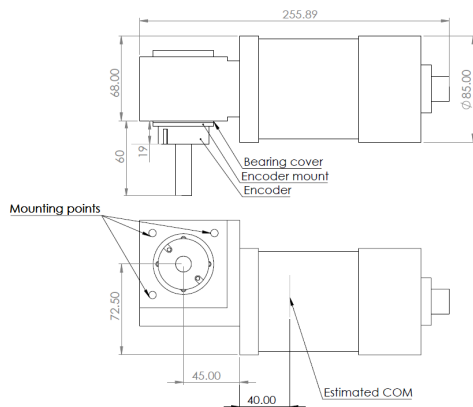


Fig. 16. Technical drawing of the motor

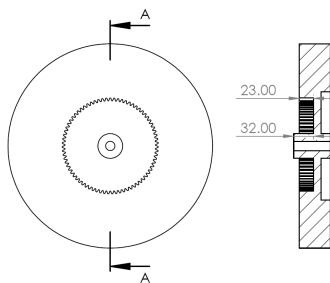


Fig. 17. Technical drawing of the wheel model

The positioning of the motor and wheel is chosen to achieve several goals:

- 1) Minimise the distance between the motor's centre of mass (COM) and the wheel axis. This in turn will minimise the distance required for mounting the batteries to balance the loading on either side of the drive axis, placing few constraints on chassis length.
- 2) The bottom plate must be kept as low as possible to ensure a low overall centre of mass while allowing

sufficient room for the chosen caster wheels (113 mm total height).

- 3) The motor should be fixed in place using the side plate, and rest on the baseplate to allow a greater weight distribution for the motors and place less strain on the mounting bolts.

As outlined in section II, the inherited spur gears and ring gears on the drive wheel require a 51 mm centre distance. Figure 18 shows the wheel mounting point relative to the output motor shaft. This geometry results in a base plate at a height of 129mm, and the motor's COM 50 mm from the wheel axis. These two factors determine the position of the batteries required to balance loads on either side of the drive axis and the length of extrusion needed to achieve the specified 1.7 m maximum height.

Figure 17 does not account for tyre width, which necessitates the use of a 5 mm spacer to reduce drag by preventing the tyres from rubbing against the side plate. Additionally, 25 mm spacers are used for the motor mount to provide clearance between the encoder and the side plate. A drawing showing the top view of the motor/wheel assembly is shown in figure 19.

To achieve goal 3, the geometry of the motor is used. The bottom edge of the side plate is flush with the top of the base plate. Ensuring the mounting points for the motor place the shaft 72.5 mm above the bottom edge of the side plate will result in the motor resting on the base plate.

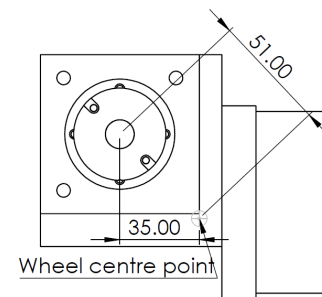


Fig. 18. Wheel mount position relative to the motor shaft

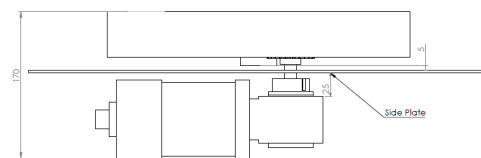


Fig. 19. Drawing of motor/wheel assembly Battery Placement

Battery Placement Balancing the mechanical load on either side of the drive axis is critical to ensure stability and minimise the risk of tipping [13]. This balancing was primarily achieved through the placement of batteries. The following considerations drove the battery placement:

- Each motor weighs 4 kg.
- Each battery weighs 3 kg.
- The COM for each motor is approximately 50 mm from the wheel axis.

- The overall width of the chassis is constrained to 610 mm, and each motor/wheel assembly contributes 170 mm to the chassis width.
- Battery dimensions shown in figure 20 are 174 mm (l), 165 mm (w), 120 mm (h).
- It is assumed the batteries have a uniform weight distribution.

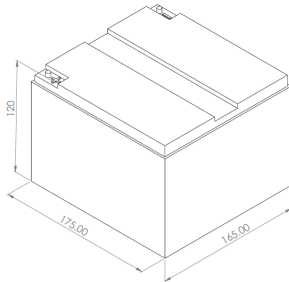


Fig. 20. Drawing showing the major dimensions of the battery

To balance the load applied by each motor, the COM for each battery must be placed 66.5 mm on the other side of the drive axis, requiring placement between the main body of each motor. The width contributed by each motor/wheel assembly allows for 270 mm of space between each motor where batteries can be mounted. Considered configurations are listed below:

- **Side-by-side:** Placing the batteries in a side-by-side configuration requires a minimum distance of 330 mm between motors, so is ruled out.
- **Stacked:** Stacking the batteries halves the required space compared with side by side, to 165 mm.
- **Sideways side-by-side:** This configuration swaps width and height dimensions, allowing batteries to be placed side-by-side within the 264 mm maximum allowable distance between motors.

Both the stacked and sideways side-by-side configurations fit within the spatial constraints. The stacked configuration allows a smaller chassis width than sideways side-by-side, however, places the COM 38 mm higher. With little advantage to reducing the chassis width below 610 mm, the sideways side-by-side configuration is chosen, shown in figure 21. To fix the batteries in place, hold-downs are used, which increase the overall battery height to 210 mm.

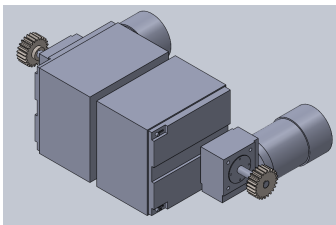


Fig. 21. Battery/motor configuration

Caster Wheel Placement

The selection of caster wheels is described in section IV, A. They have a 75 mm wheel diameter, with a 113 mm overall

height. The mounting plate is 98 mm x 79 mm, with four 9 mm mounting holes spaced 80 mm x 60 mm. Placement of the caster wheels is done to ensure mounting points do not clash with batteries, allowing at least 20 mm of clearance. Figure 22 gives a drawing of the base plate, showing the position of motors, batteries, and mounting points for caster wheels.

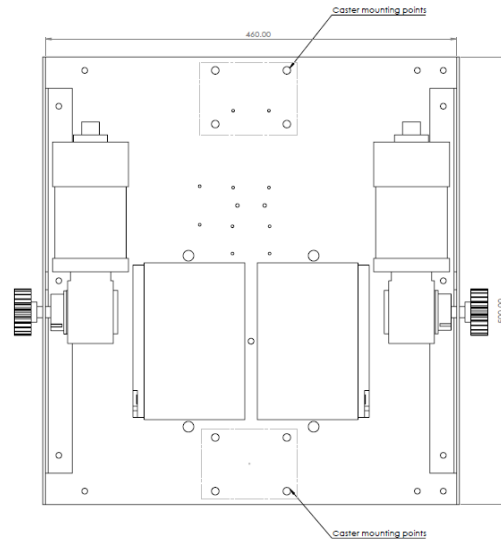


Fig. 22. Chassis base plate

Aluminium Frame

The torso contributes 1 m to the height, the top plate and base plate are each 3 mm thick. The base plate is 129 mm above the ground. To obtain the 1.7 m total height requires that the height of the aluminium frame is 565 mm. Length run extrusion at the bottom of the frame will clash with the motors, so angle bar is used in its place. Figure 23 shows a Solidworks assembly of the chassis structure. The side plate is made transparent in this figure to show the position of the motor. Note that the side plate runs the length of the chassis.

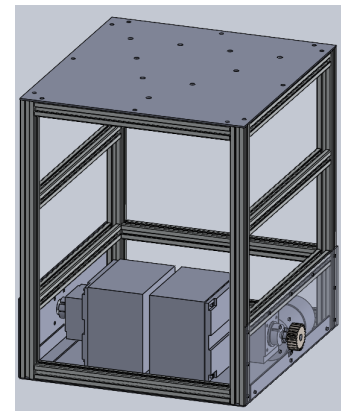


Fig. 23. Chassis structure

Electronics Incorporation

To facilitate the incorporation of electronics, laser-cut acrylic is used. A switch mount back plate is implemented which houses the motor main switch and emergency stop assembly, an access point for the motor fuse. A shelf assembly

is used to house the PSU, TCB and RGB LED control board, the sensor board, NUC, NUC power supply, and PSD sensors. Each laser-cut part contains holes to allow for cable management via cable ties. Laser-cut "cable risers" are also added to the side so cables can easily be run between shelves and the base plate. Figure 24 shows a full Solidworks assembly with these components incorporated.

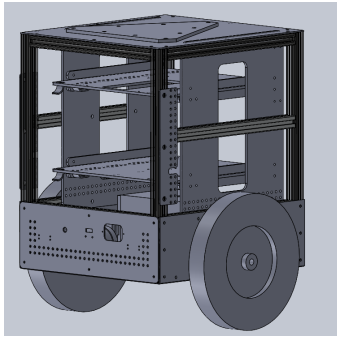


Fig. 24. Complete chassis assembly

Ultrasonic sensor mounts make use of the modularity provided by aluminium extrusion, using a single design that can be mounted anywhere there is free space on the aluminium extrusion, figure 25 shows three ultrasonic sensors mounted to the chassis in different ways.

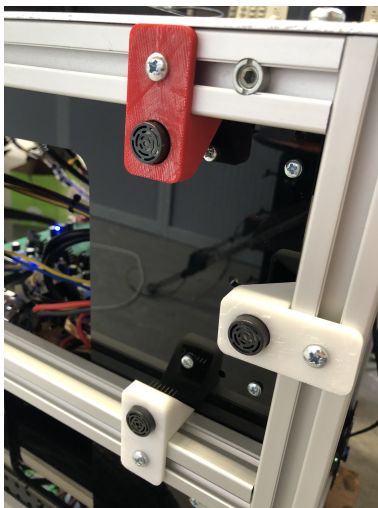


Fig. 25. Ultrasonic sensor mounts

Summary

The design and implementation of the chassis for MARVIN encompasses a range of specifications, constraints, and considerations to create a stable and adaptable foundation. T-slot extruded aluminium is chosen as the primary material, adopting a modular bolt-together approach. The design prioritises achieving the desired centre of mass (COM) location, minimising chassis base height, and ensuring access to critical components. Careful placement of batteries, caster wheels, and the incorporation of electronics further enhance the functionality and overall performance of the chassis. This design process contributes to MARVIN's robust and adaptable chassis, setting

the stage for future developments. An image of MARVIN fully assembled is shown in figure 26.



Fig. 26. MARVIN assembled

D. Software

This section covers the design and implementation of the project's software components. It explores the rationale behind selecting Python as the primary programming language, the use of the ROS2 framework, and the structure used to control MARVIN. Additionally, it outlines the communication protocol implemented for data exchange between the NUC and the sensor board.

1) Programming Languages: Python is chosen as the primary programming language for the robotic system due to its simplicity and rapid development capabilities. Its ease of use allows for quick prototyping and development, making it an ideal choice for getting things up and running efficiently.

C++ is also used, primarily for the Arduino platform. This choice is driven by the need to program an Arduino microcontroller used for the sensor board, described in section II, which is typically programmed in C++ [32].

2) Choice of ROS2 Framework: ROS2, the Robot Operating System 2 [33], is selected as the framework upon which to build MARVIN's software. The decision to use ROS2 is based on several key advantages:

- **Nodes and Topics Structure:** ROS2 utilises a node-based architecture where each node represents a distinct component or task within the system [33]. Nodes communicate via topics, which are named message queues, allowing for efficient data exchange. ROS2 nomenclature refers to the information conveyed over topics as messages, where nodes can publish or subscribe to topics. This structure promotes modularity and scalability in the system's design. Nodes can be easily added or modified without affecting the entire system.
- **Support for SLAM:** ROS2 offers packages and libraries that enable Simultaneous Localisation and Mapping (SLAM), a crucial technology for mapping and understanding the robot's environment. SLAM allows the

robot to create maps of its surroundings and simultaneously determine its position within those maps.

- **Support for Autonomous Navigation:** ROS2 provides tools and libraries for autonomous navigation, enabling robots to plan and execute movements in their environments. This support allows your robot to make decisions and navigate without constant human intervention.

The choice of ROS2 aligns with the principles of sustainability, emphasising efficiency, modularity, and the establishment of a strong foundation for future developments.

3) **Description of ROS2 Network:** Two fundamental packages that come with ROS2, namely Joy and Teleop Twist Joy, play key roles in this network, allowing for manual control. These packages facilitate the integration of a generic Bluetooth controller, with the ROS2 ecosystem. A breakdown of the essential components and their functionalities within the ROS2 network built for this project follows, figure 27 shows a block diagram of the network and how it interfaces with external devices:

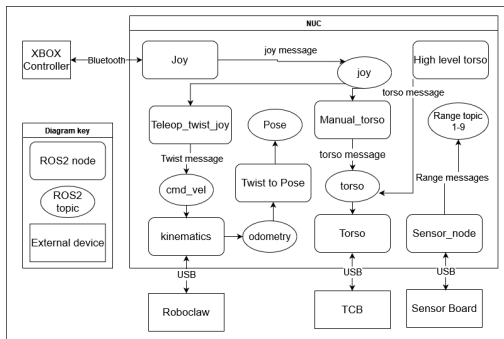


Fig. 27. Block diagram of ROS2 network

- **Joy and Teleop Twist Joy:**

- **Joy:** This package serves as an interface between a generic Bluetooth controller, including a Bluetooth XBOX controller, and ROS2 [33]. It publishes button presses as joy messages to the joy topic. This existing package and familiarity with an XBOX controller drove the choice to use an XBOX controller to execute manual control.
- **Teleop Twist Joy:** Subscribes to joy messages and converts button press information into velocity commands. These commands are published as Twist messages to the cmd_vel topic, containing linear and rotational velocity information.

- **Kinematics Node:** This node acts as an interface between the Roboclaw motor driver and ROS2. It subscribes to the cmd_vel topic and publishes timestamped Twist messages to the encoder topic. These Twist messages are used to inform ROS about MARVIN's speed, as opposed to the cmd_vel Twist messages which are used as velocity commands. Kinematic calculations are shown in section IV, A.
- **Twist to Pose Node:** This node handles odometry and is placed immediately after the Kinematics Node. It subscribes to the encoder topic, where the Kinematics

Node publishes Twist messages. By integrating these Twist messages over time, the Twist to Pose node keeps track of MARVIN's pose relative to its starting pose.

- **Torso Messages:** Torso messages are used to enable torso control, they are custom messages that contain a string command and integer setpoint.
- **Torso Node:** The Torso node is an interface between ROS2 and the Torso Control Board (TCB). It subscribes to the torso topic, receiving torso messages. It uses these messages to call the appropriate functions in the torso interface, thereby controlling MARVIN's torso. To facilitate manual control, this node interprets setpoints outside of the range [0, 255] as instructions to increase or decrease the actuator value, figure 28 illustrates this.
- **Manual Torso Node:** The Manual Torso Node demonstrates an example of multiple nodes subscribing to the same topic while executing different tasks. It subscribes to the joy topic, interprets button presses, and publishes torso messages to the torso topic.
- **High-Level Torso Node:** The High-Level Torso Node serves as a testbench for the torso functionality. It iterates through each torso actuator, providing a minimum, mid, and maximum setpoint before moving to the next. This node is shown in figure 27 to illustrate the design's adaptability, allowing for the use of the robot's torso without needing to change the core Torso node. Importantly, it is not used concurrently with Manual Torso.
- **Sensor Node:** The Sensor Node acts as an interface between ROS2 and a sensor board. Using a library of sensor interface functions, this node periodically polls the sensor board for sensor data. It then publishes each range value onto separate topics, making this information available for navigation, perception, or other relevant tasks.

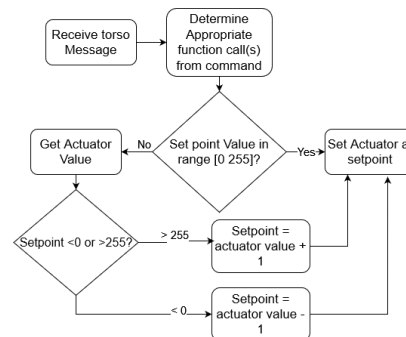


Fig. 28. Block diagram of Torso node

4) **Communication with Sensor Board:** Basic firmware is required for the Arduino to control the sensor board and interface with the NUC running ROS2. The firmware makes use of a communication protocol based on the inherited torso interface and the Roboclaw interface [24]. Table I shows the structure of data packets used for sensor communication. Packets received by the sensor board typically contain only 1 byte in the data section which gives the sensor type from which readings are being requested. Packets sent by the sensor board contain readings from each sensor within the data bytes

using the structure shown in table II. Lastly, byte stuffing is implemented by inserting an escape byte before any data bytes equal to the start, escape, or end bytes. This protocol ensures reliable and error-checked communication between the Arduino-based sensor board and the ROS2 system.

TABLE I
PACKET STRUCTURE FOR THE SENSOR INTERFACE

Start	1 byte
Data	1 to 40 bytes
Checksum	1 byte
End	1 byte

TABLE II
STRUCTURE OF SENSOR DATA BYTES

Sensor type	Sensor number	upper byte	lower byte
-------------	---------------	------------	------------

Recall from section II, inherited sensors are four PSD sensors which range continuously, and five ultrasonic sensors which require a signal to trigger a reading, and will send a signal when range data is ready to be read. A more detailed description of each sensor, and how they connect with the sensor board is given in section II.

Figure 29 shows the process undergone by the sensor board upon receipt of a valid packet. Packets are sent 1 byte at a time, with byte stuffing occurring as the packet is sent. A timeout while waiting for ultrasonic readings indicates that at least 1 sensor has stopped responding to trigger signals. Additionally, The ultrasonic response signal is attached to an interrupt, which will set an ultrasonic error status if no reading has been triggered.

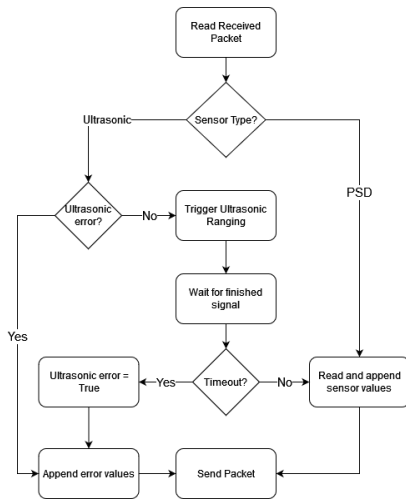


Fig. 29. Block diagram of sensor board process

5) **Summary:** To summarise, this subsection has outlined the fundamental elements of the software design. Python is selected as the primary programming language for its simplicity and rapid development capabilities, while the specific ROS2 framework is chosen to form the foundation of the software architecture. Within this framework, a tailored network structure is introduced, designed specifically for the project's requirements. Together with the communication protocols, these

elements shape the software design for MARVIN's operation, ensuring an adaptable foundation for future maintainers and developers.

V. EVALUATION

Testing is conducted on MARVIN to verify functionality and performance. This section outlines the methodology and results for tests conducted on MARVIN. It is important to note that before conducting any mobile evaluation, one of MARVIN's batteries failed, and a power supply set to 26.2 V was used in place.

A. Mass

When fully assembled, MARVIN is weighed using scales, and a mass of 63.5 kg is measured, corresponding to a weight force of 623 N.

B. Chassis Strength

Before installing the 23 kg torso assembly, the drive chassis was tested for strength and rigidity by applying different loads. While a maximum load is not determined, the drive chassis is observed to support at least 90 kg without exhibiting any bending or flexing.

C. Stability

Stability is evaluated using a tip test to estimate the height of MARVIN's COM. MARVIN is tipped sideways until a balance point is found, where the COM will be directly above the contact point with the ground. Figure 30 shows a diagram of how this test is conducted. The figure only shows drive chassis geometry, however, testing is conducted with the torso assembly installed. It is found that MARVIN has a critical tipping angle of 62.5°, corresponding with a 586 mm COM height.

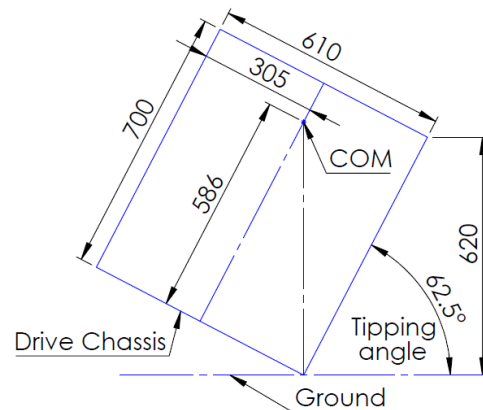


Fig. 30. Diagram of tipping test conducted on MARVIN

The right angle triangles formed between MARVIN's wheels and COM are shown in figure 31. MARVIN's weight force is applying 190 Nm torque at the ground contact point of each drive wheel, and 155 Nm at each caster wheel. To tip MARVIN, a force must be applied that applies a greater

torque on a given contact point than is applied by MARVIN's weight force [34]. It is determined a horizontal force of 325 N is required to tip MARVIN sideways, enabling a curved path with up to 5 ms^{-2} centripetal acceleration, at 1.4 ms^{-1} tangential velocity, this corresponds to a turning radius of 392 mm, these figures are found using Eq. 5 [35]. To tip MARVIN forwards or backwards or forwards, a horizontal force of 265 N is required, enabling 4 ms^{-2} acceleration. This means that MARVIN can theoretically come to a complete stop in less than 0.5 s when travelling at 1.4 ms^{-1} .

$$a_c = v^2/r. \quad (5)$$

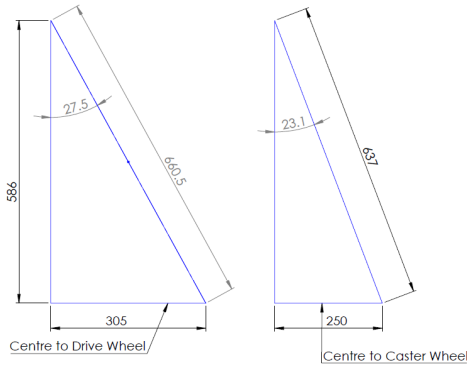


Fig. 31. Right angle triangles formed between wheel contacts and MARVIN's COM

D. Stopping Distance

Stopping distance is assessed using both a hardware and software emergency stop. The hardware disconnects the main battery connection of the Roboclaw, causing MARVIN to freewheel until it comes to a complete stop. A software emergency stop gives the Roboclaw a 0 setpoint speed for each motor. Testing is conducted for both slow and medium to fast walking paces, on both carpet and vinyl. Table III gives the maximum recorded stopping distance in each case.

TABLE III
MARVIN STOPPING DISTANCES

	Carpet		Vinyl	
	Software	Hardware	Software	Hardware
Slow pace	0.26 m	0.95 m	0.32 m	1.1 m
Medium/fast	0.86 m	2.2 m	0.8 m	1.37 m

E. Power Consumption

Evaluation power consumption had a primary focus on the power drawn by the motors while in motion. Initially, this was to be conducted using the current reading from the Roboclaw, which gives current directly to each motor, then estimating current from the battery using the duty cycle. The Roboclaw current readings are found to be unreliable through a test that compares an ammeter reading to the average Roboclaw reading given while operating MARVIN on blocks, driving the

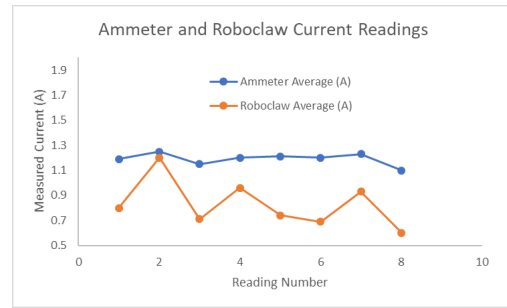


Fig. 32. Plot comparing Ammeter readings to Roboclaw current readings

wheels at their medium/fast pace rate. Figure 32 shows a plot of ammeter readings with their associated Roboclaw reading.

A current clamp is used to measure the current to each of MARVIN's motors, as well as directly to the motor driver while in motion. Video recordings of the measurement are taken due to rapid changes in readings that occur during motion. Current readings are obtained by reviewing the footage. Testing is conducted on both vinyl and carpet, for both slow and medium/fast paces. Figure 33 shows the mean current in each test condition, with error bars giving the standard deviation of these measurements. Additionally, with all components on, an idle current of 1 A is measured. Allowing for a 30% safety margin, this data shows that MARVIN can achieve an 8-hour run time with up to 25% of time spent in motion in the highest power demand case.

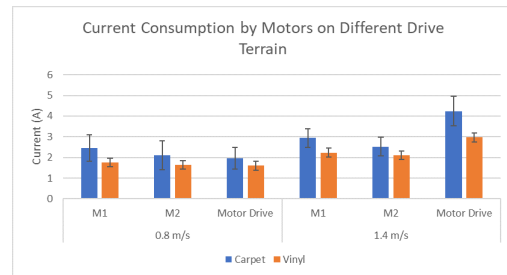


Fig. 33. Current consumption by motors while MARVIN is in motion

F. Odometry Drift

MARVIN's odometry is measured by driving MARVIN forward approximately 8 m and measuring the lateral translation, as well as the forward distance of each wheel. Figure 34 gives a visual representation of these measurements. By taking the lateral movement, and the difference between the left and right wheel forward distance, the position and orientation (pose) of MARVIN can be calculated, and compared with the ROS2 system estimate of MARVIN's pose based on odometry data.

Testing revealed that when instructed to move forward (in the Y direction), MARVIN exhibits a small positive (anticlockwise) Z-axis rotational velocity, thus veers left. This shows that the forward velocity contributed by the left wheel is less than that contributed by the right wheel. This effect is observed over a range of velocities.

Figures 35, 36, and 37 show the ROS2 odometry estimate of position with the measured position. In most cases, odometry

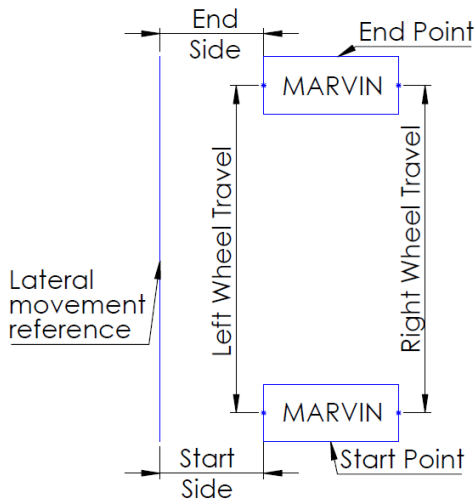


Fig. 34. Diagram showing method of testing odometry

over the estimated forward distance travelled, with less than 100 mm error, however, this would wind up over time. The difference in measurement 8 is due to the skidding that occurred when coming to a stop. X distance and angle differ greatly between the measured value and odometry estimate, this discrepancy may be explained by the noise present on the right motors speed measurements, shown in figure 38, measured with a 0 quadrate pulses per second (QPPS) setpoint.

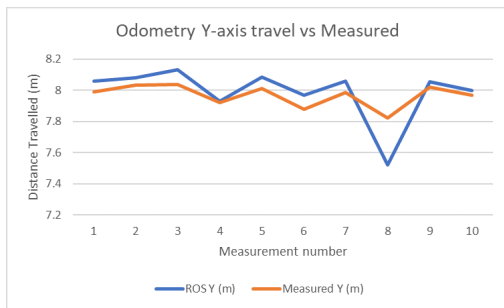


Fig. 35. Y distance travelled - Odometry estimate vs measured

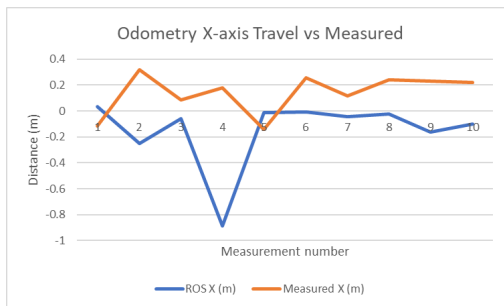


Fig. 36. X distance travelled - Odometry estimate vs measured

VI. FUTURE WORK

A. Regenerative Braking

Working on regenerative braking is a continuation of the project's sustainability goals relating to energy efficiency. It

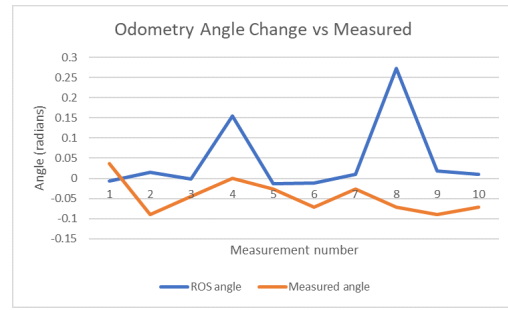


Fig. 37. Z angle change - Odometry estimate vs measured

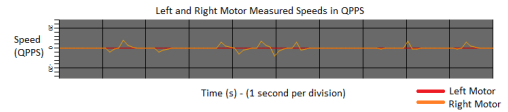


Fig. 38. Left and right motor speeds with 0 QPPS setpoint

would also improve MARVIN's safety, as this allows braking to occur when the hardware emergency stop is used, which will reduce stopping distance. While the batteries implemented into the design have internal cell balancing circuitry [23], charging them in their series configuration can cause the batteries to become unbalanced. [36] shows some methods for charge balancing, including a charge shuttle, which uses capacitors to shuttle charge between batteries.

B. Protection Circuitry

Additional protection circuitry is required to ensure the batteries remain functional.

C. Locomotion Control

Locomotion control needs improvement. The implemented odometry is observed to have large errors in estimating orientation, and x-axis travel (on a global reference). This may be improved by taking encoder counts at each wheel and determining the distance travelled by the rotation of each wheel between samples, rather than integrating velocity over time. Additionally, MARVIN is observed to veer left when instructed to move forward. Presently closed-loop control is only implemented for motor speeds, however small differences between each wheel, such as tread, inflation, or camber, can make it difficult to ensure a differential drive robot operates exactly in the way it is commanded [13]. Additional feedback should be implemented to measure MARVIN's actual velocity and compare it against the set point given. For example, a gyroscope can be used to measure z-axis rotation and alter wheel speeds to compensate for error.

D. SLAM and Autonomous Navigation

Where locomotion control is implemented, SLAM and autonomous navigation can follow. Safety must be greatly considered in this area. With a 0.86 m maximum software stopping distance observed, MARVIN must be capable of

executing an emergency stop if unexpected obstacles are detected within this distance plus a safety margin. If a 1.5 m distance is used for an emergency stop, MARVIN's range sensors must have a latency of less than 700 ms to ensure an emergency stop is executed greater than 1 m away from the detected obstacle.

VII. CONCLUSION

The completion of this project has enabled MARVIN to transform a non-functional state, into a fully functionality, mobile robotic platform. MARVIN offers a runtime comparable to similar HRI platforms and has proven performance in terms of velocity, power consumption, safety, and strength. The software component of this project has enabled successful interfacing with torso control, implementing manual control of the torso with the use of an abstraction layer enabling future developers to use the torso differently, without changes to the ROS2 torso node. Additionally, sensor interfacing is implemented, allowing accurate communication with a sensor board, and range sensor data to be published into MARVIN's ROS2 network.

With a sustainability focus on energy efficiency, re-use, and modularity, MARVIN stands at the end of this project as an eco-conscious tool, providing a solid foundation for future developments.

REFERENCES

- [1] R. Kitchen, "University's robot learns how to be a human," *Dominion Post*, 2009.
- [2] D. Carnegie, "Robotics in a new age," *Victorious*, 2006.
- [3] D. Thomson, "Hybrid control of a segway platform developed in mrds," 2013.
- [4] D. Loughnane, "Design and construction of an autonomous mobile security device," 2001.
- [5] T. Exley, "Personal correspondence," 2023.
- [6] Unknown, "Our sustainability," 2022. [Online]. Available: <https://environment.govt.nz/about-us/our-sustainability/#:~:text=renewing%20our%20sustainability%20strategy%20to,2030%20from%202017/18%20levels>
- [7] E. M. M. et al, "Outdoor walking speeds of apparently healthy adults: A systematic review and meta-analysis," *Springer Sports Meidicine*, 2020.
- [8] C. J. Robinson, "Autonomous operation and human-robot interaction on an indoor mobile robot," 2016.
- [9] *DC-DC Converters Bus Converter.Power Module Type Instruction Manual*, Cosel.
- [10] "Lv-maxsonar-ez datasheet," Datasheet, MaxBotix, 2005.
- [11] "Device speicification for gp2y0d21yk0f," Datasheet, 2009.
- [12] B. de Bakker. (2019) How to use a sharp gp2y0a710k0f ir distance sensor with arduino. [Online]. Available: <https://www.makerguides.com/sharp-gp2y0a710k0f-ir-distance-sensor-arduino-tutorial/>
- [13] R. Siegwart *et al.*, *Introduction to Autonomous Mobile Robots*. MIT Press, 2011.
- [14] unknown. (2023) Robots - 2 legs or wheels. which is better. [Online]. Available: <https://www.unlimited-robotics.com/post/robots-2-legs-or-wheels-which-isbetter#:~:text=Wheeled%20robots%20are%20designed%20to,and%20easily%20over%20smooth%20surfaces>
- [15] A. Hughes and B. Drury, *Electric Motors and Drives - Fundamentals, Types and Applications (5th Edition)*. San Diego: Elsevier, 2019.
- [16] S. H. Kim, "Electric motor control: Dc, ac, and bldc motors," *Elsevier Science Technology*, 2017.
- [17] Unknown. Motor encoder overview. [Online]. Available: https://www.dynapar.com/technology/encoder_basics/motor_encoders/
- [18] I. Lab. (2010) Photo of jenny. [Online]. Available: <http://isrlab.tistory.com/34>
- [19] S. C. et al, "Ari: the social assistive robot and companion," *IEEE International Conference on Robot and Human Interactive Communication*, 2020.
- [20] W. X. L. Xie, C. Scheifele and K. A. Stol, "Heavy-duty omni-directional mecanum-wheeled robot for autonomous navigation: System development and simulation realization," *IEEE International Conference on Mechatronics (ICM)*, 2015.
- [21] Unknown. (2023) diff_drive_controller. [Online]. Available: http://wiki.ros.org/diff_drive_controller
- [22] ——. (March 8, 2023) Lifepo4 vs. lithium ion batteries: What's the best choice for you? [Online]. Available: <https://blog.ecoflow.com/us/lifepo4-vs-lithium-ion-batteries>
- [23] Powertech, "SB2213 LiFePO₄Battery."
- [24] *Roboclaw Series User Manual*, BasicMicro.
- [25] *H6 Series Incremental Magnetic Encoder*, Phoenic America.
- [26] Rolling resistance. [Online]. Available: https://www.engineeringtoolbox.com/rolling-friction-resistance-d_1303.html
- [27] Unknown, "Push-pull forces of wheeled equipment on selected carpets: A report for interface australia," *Dohrmann Consulting*, 2016.
- [28] C. A. Rusen, "Intel nuc10i5fnh review: Solid performance in a small form factor!" Digital Citizen, Tech. Rep., 2020. [Online]. Available: <https://www.digitalcitizen.life/intel-nuc10i5fnh-review/>
- [29] Unknown. (2019) Average height and wight by country. [Online]. Available: <https://www.worlddata.info/average-bodyheight.php>
- [30] "Transpower." [Online]. Available: <https://transpower.co.nz/>
- [31] A. Reni, "Personal correspondence," 2023.
- [32] Arduino. (Year of publication, e.g., 2023) Getting started with arduino. [Online]. Available: <https://www.arduino.cc/en/Guide/HomePage>
- [33] ROS 2. (Year of publication, e.g., 2023) ROS 2 Tutorials. [Online]. Available: <https://index.ros.org/doc/ros2/Tutorials/>
- [34] J. K. N. Richard G. Budynas, *Shigley's Mechanical Engineering Design*. McGraw-Hill, 2008.
- [35] G. A. DiLisi, *Classical mechanics. Volume 3, Newton's laws and uniform circular motion*. San Rafael California, 2019.
- [36] Y. Barsukov, "Battery cell balancing: What to balance and how," *Texas Instruments*, unknown.